Supplementary Information

Sea-ice thickness initialization improves summertime sea ice prediction in the Barents-Kara Sea

Yushi Morioka[1], Doroteaciro Iovino[2], Andrea Cipollone[2], Andrea Storto[3],
Takeshi Doi[1], Masami Nonaka[1], Swadhin K. Behera[1]

1: Japan Agency for Marine-Earth Science and Technology
2: Institute for Earth System Predictions, CMCC
3: Institute of Marine Sciences, CNR

27 Aug 2026 (Revised)
The Cryosphere

Corresponding Author: Yushi Morioka
Showamachi 3173-25, Kanazawa-ku, Yokohama, JAPAN
morioka@jamstec.go.jp, +81-45-778-5509

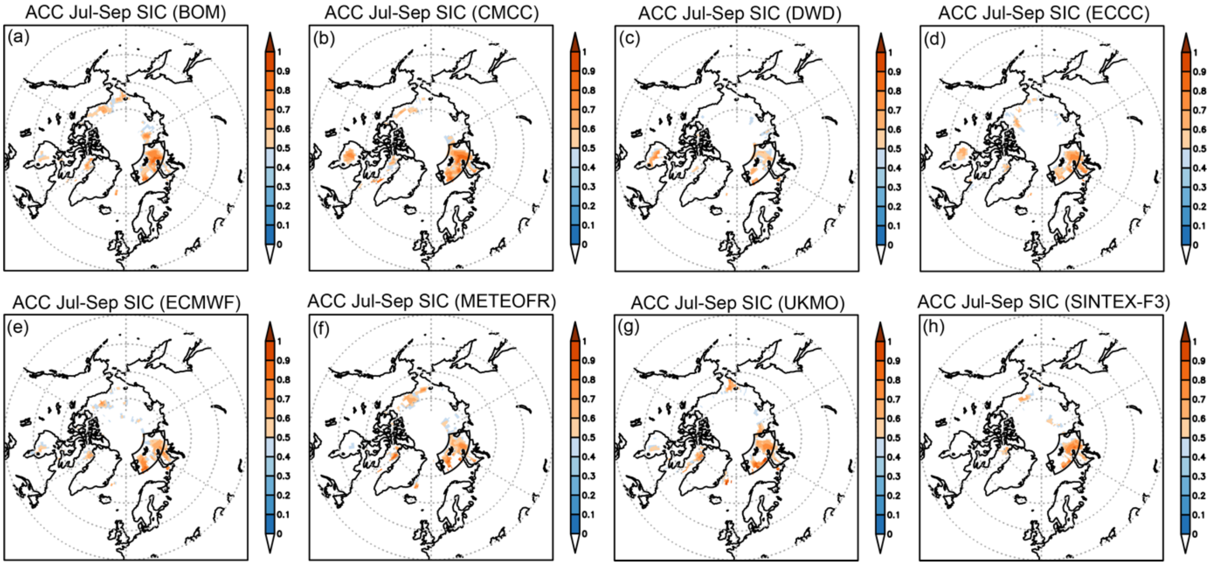

Figure S1: (a) Anomaly correlation (ACC) of July-September mean SIC in the Arctic Ocean during 1993-2016 between the observation data (NSIDC) and the prediction results from BOM. Color indicates ACC that is statistically significant at 95 % using Student's *t*-test and exceeds the ACC of the persistence prediction based on the observation. (b-h) Same as in (a), but for the prediction results from CMCC, DWD, ECCC, ECMWF, METEOFR, UKMO, and SINTEX-F3 models, respectively.

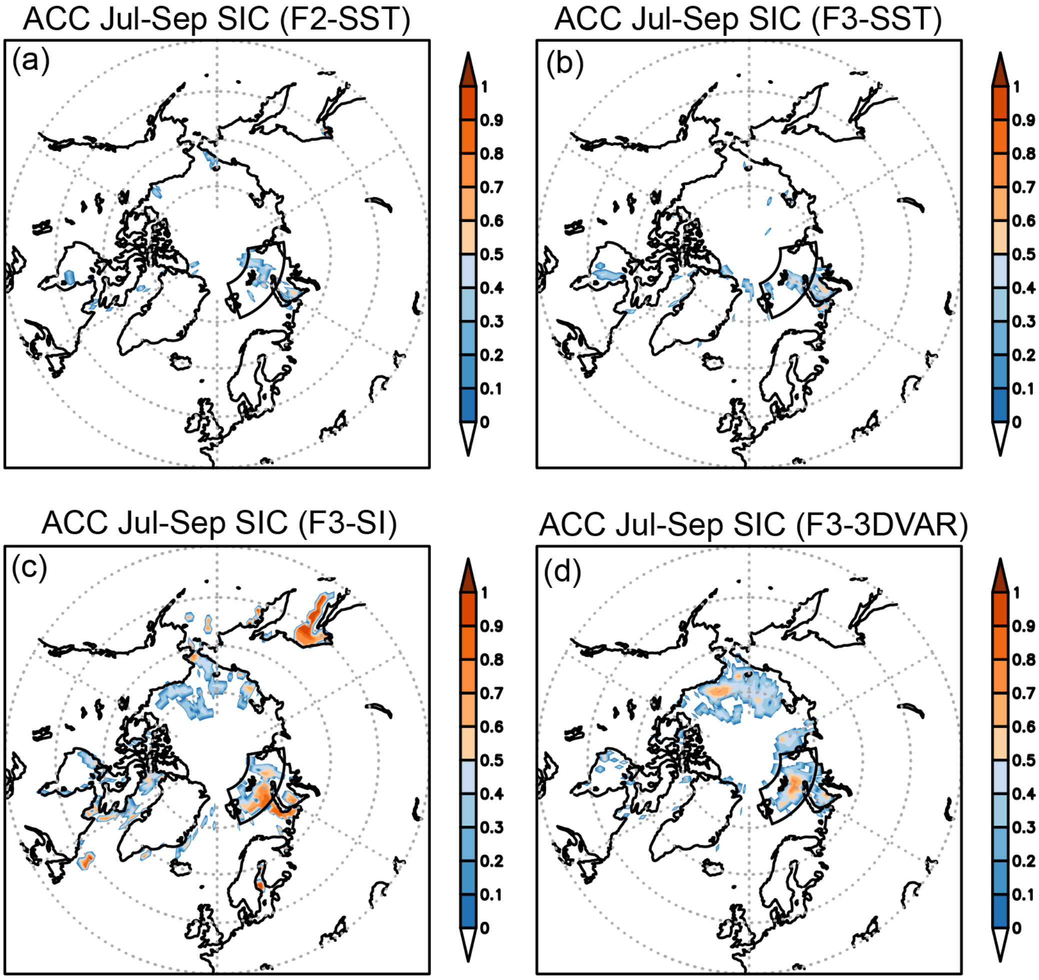

Figure S2: (a) Anomaly correlation (ACC) of July-September mean SIC in the Arctic Ocean during 1982-2022 between the observation data (NSIDC) and the prediction results from SINTEX-F2 with SST initialization (F2-SST). Color indicates ACC that is statistically significant at 95 % using Student's *t*-test and exceeds the ACC of the persistence prediction based on the observation. (b-d) Same as in (a), but for the prediction from SINTEX-F3 with SST initialization (F3-SST), with SST and sea ice initializations (F3-SI), and with SST, sea ice, and subsurface ocean initialization using 3DVAR approach (F3-3DVAR), respectively.

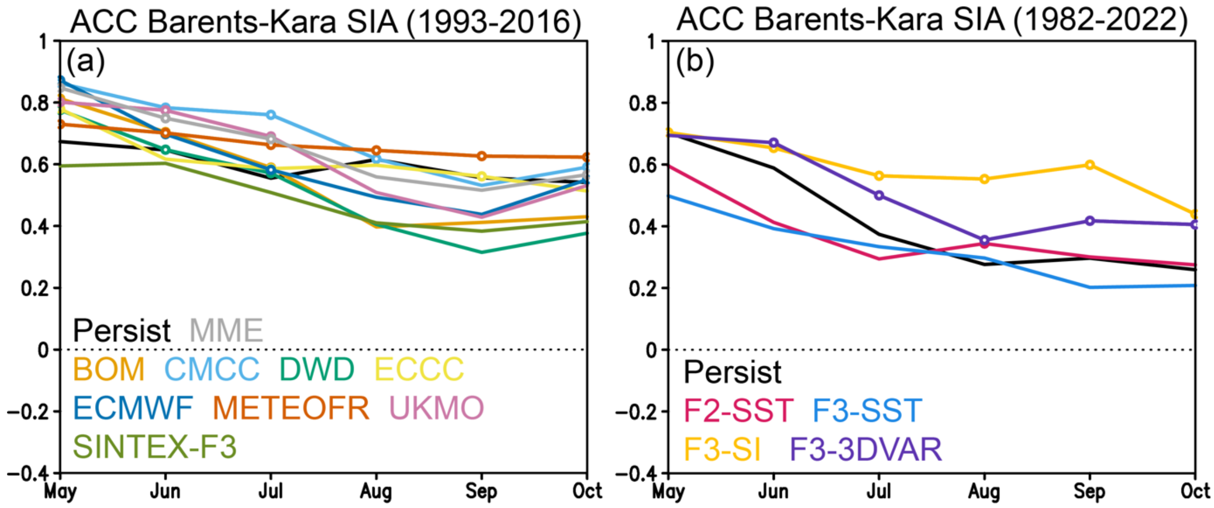

Figure S3: (a) Anomaly correlation (ACC) of Barents-Kara SIA during 1993-2016 between the observation (NSIDC) and the prediction from the multi-model ensemble mean C3S (MME) and the ensemble mean BOM, CMCC, DWD, ECCC, ECMWF, METEOFR, UKMO, and SINTEX-F3. Persistence prediction skills are shown in black. Open circles indicate ACCs that are statistically significant at 95 % using Student's *t*-test and exceed the ACCs of the persistence prediction based on the observed SIA. (b) Same as in (a), but for the ensemble mean SIA during 1982-2022 from SINTEX-F2 with SST initialization (F2-SST), SINTEX-F3 with SST initialization (F3-SST), SINTEX-F3 with SST and sea ice initializations (F3-SI), and SINTEX-F3 with SST, sea ice, and subsurface ocean initializations using 3DVAR approach (F3-3DVAR).

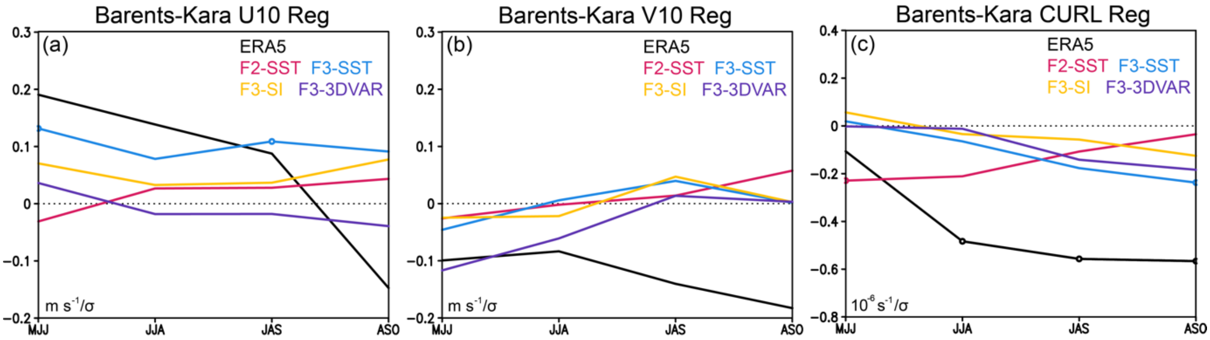

Figure S4: (a) Barents-Kara zonal wind speed anomalies at 10 m (U10; in m s^{-1}/σ) regressed on July-September mean standardized Barents-Kara SIE index during 1982-2022. The reanalysis from ERA5, the ensemble mean regressions from SINTEX-F2 with SST initialization (F2-SST), SINTEX-F3 with SST initialization (F3-SST), SINTEX-F3 with SST and sea ice initializations (F3-SI), and SINTEX-F3 with SST, sea ice, and subsurface ocean initializations using 3DVAR approach (F3-3DVAR) are shown, respectively. Here we show the slope of linear regression as the regression value. Open circles indicate regression values that are statistically significant at 95 % using Student's *t*-test. (b-c) Same as in (a), but for Barents-Kara meridional wind at 10 m (V10; in m s^{-1}/σ) and wind curl at 10 m (CURL; in 10^{-6} m s^{-1}/σ) regressions.

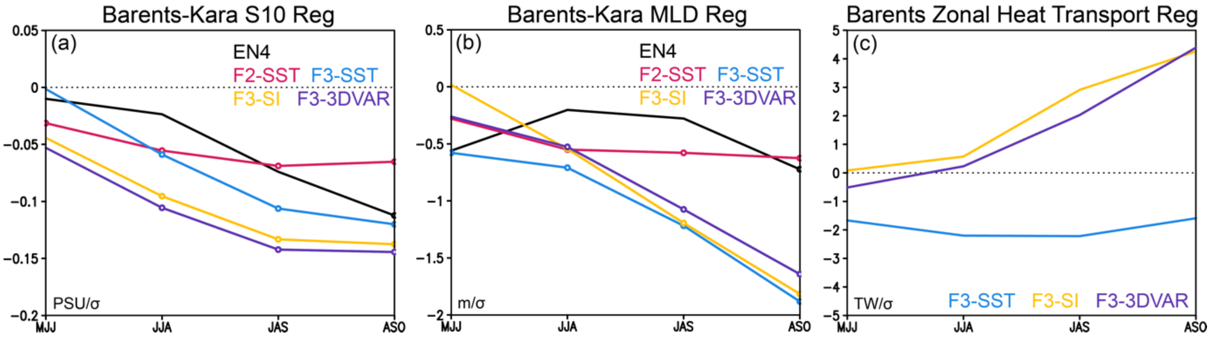

Figure S5: (a) Barents-Kara salinity anomalies at 10 m depth (S10; in PSU/ σ) regressed on July-September mean standardized Barents-Kara SIE index during 1982-2022. The observation from EN4, the ensemble mean regressions from SINTEX-F2 with SST initialization (F2-SST), SINTEX-F3 with SST initialization (F3-SST), SINTEX-F3 with SST and sea ice initializations (F3-SI), and SINTEX-F3 with SST, sea ice, and subsurface ocean initializations using 3DVAR approach (F3-3DVAR) are shown, respectively. Here we show the slope of linear regression as the regression value. Open circles indicate regression values that are statistically significant at 95 % using Student's *t*-test. (b-c) Same as in (a), but for Barents-Kara mixed-layer depth (MLD; in m/ σ) and zonal heat transport at Barents Sea Opening (BSO; in TW/ σ) regressions. Note that due to the data availability, the BSO heat transport regressions from EN4 and SINTEX-F2 are not shown in (c).

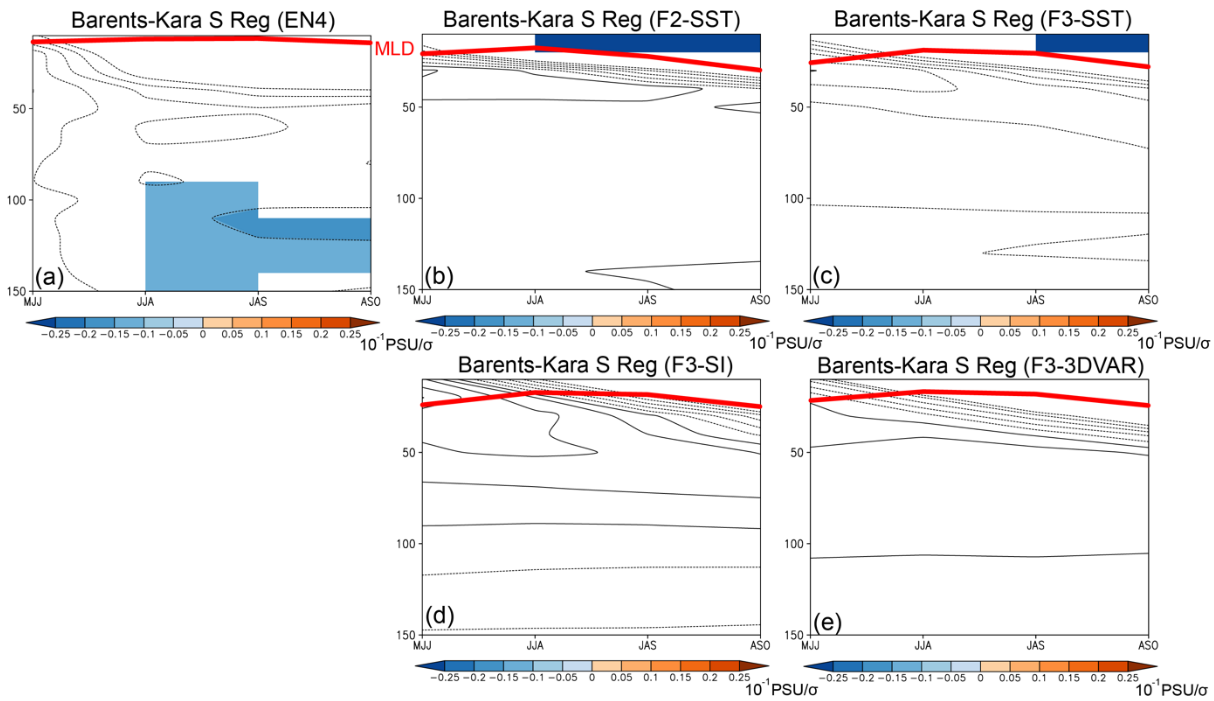

Figure S6: (a) Barents-Kara subsurface ocean salinity anomalies (T; in 10^{-1} PSU/ σ) from EN4 regressed on July-September mean standardized Barents-Kara SIE index during 1982-2022. Color indicates regression values that are statistically significant at 95 % using Student's *t*-test. Red solid line corresponds to the mixed-layer depth (MLD) at which the ocean potential density increases by 0.03 kg m^{-3} from the one at 10 m depth. (b-e) Same as in (a), but for the ensemble mean regressions from SINTEX-F2 with SST initialization (F2-SST), SINTEX-F3 with SST initialization (F3-SST), SINTEX-F3 with SST and sea ice initializations (F3-SI), and SINTEX-F3 with SST, sea ice, and subsurface ocean initializations using 3DVAR approach (F3-3DVAR) are shown, respectively.

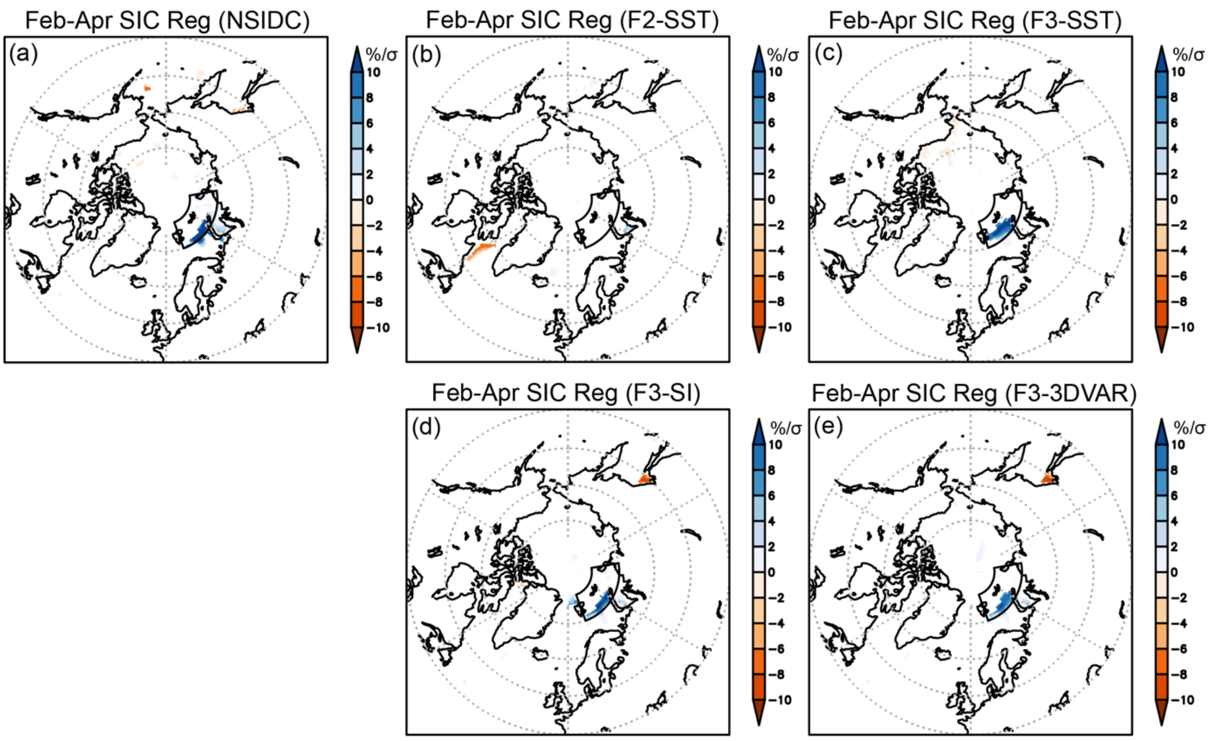

Figure S7: (a) February-April mean SIC anomalies (in %/ σ) regressed on July-September mean standardized Barents-Kara SIE index during 1982-2022 from the NSIDC. Color indicates regression values that are statistically significant at 95 % using Student's *t*-test. (b-e) Same as in (a), but for the ensemble mean SIC regressions from SINTEX-F2 with SST initialization (F2-SST), SINTEX-F3 with SST initialization (F3-SST), SINTEX-F3 with SST and sea ice initializations (F3-SI), and SINTEX-F3 with SST, sea ice, and subsurface ocean initializations using 3DVAR approach (F3-3DVAR), respectively.